A coupled approach to compute approximate solutions of a compressible immiscible three-phase flow model with fast transient and stiff source terms

Jean-Marc Hérard, Guillaume Jomée

A coupled approach to compute approximate solutions of a compressible immiscible three-phase flow model with fast transient and stiff source terms

Jean-Marc Hérard (1,2), Guillaume Jomée (1,2)

(1) EDF Lab Chatou, 6 quai Watier, 78400, Chatou, France
(2) Institut de Mathématiques de Marseille, Technopôle Château-Gombert 39, rue Frédéric Joliot-Curie 13453 Marseille Cedex 13, France

May 31, 2024

Abstract

This paper aims at developing a new numerical coupled approach to compute solutions of a compressible immiscible three-phase flow model with stiff source terms. The targeted applications involve flows with fast transient and shock waves. Thus, a well-posed model with respect to the initial conditions that embarks an entropy inequality is considered. A preliminary work on the underlying relaxation process of the model is conducted. Then the new numerical scheme is presented and numerically tested.

Introduction

This work tackles the simulation of three-phase flows with immiscible phases. More precisely, it focuses on three-phase flows with a fast transient regime. Such flows can arise in some nuclear safety scenario studies. In these cases, the considered flows are usually initialized with a huge disequilibrium between phases and this disequilibrium has a significant role in the dynamics of the flow throughout time. Actually, we know that the simulation of a three-phase flow with the assumption of instantaneous return to equilibrium between phases, such as the one conducted in [6], is unable to compute a value of the total pressure close to the one measured in [32]. Thus, it motivates the development of numerical methods that can compute solutions of three-phase flow model in full disequilibrium. The methodology developed in the sequel is an extension of the one proposed in [29] in the framework of immiscible compressible two-phase flow model belonging to the class of [1] (we refer the readers to references [13, 2, 21, 19, 23, 18, 14] for the two-phase flow framework).

More precisely, the present work concerns some innovative numerical strategy in order to handle numerical approximations of solutions of the immiscible three-phase flow model introduced in [25], extended to an undetermined number of phase in [24], and partially investigated in [6]. The latter model aims at computing velocities, temperatures, pressures and statistical fractions of an eleven-equation model. The mass, momentum and energy balance equations are written for each phase, and they are complemented by two PDEs corresponding to the governing equations of statistical fractions. Obviously, EOS must be introduced within each phase, and closure laws must be defined in order to account for interfacial transfers between phases. In practice, since shock patterns arise in the considered flows, the model must be such that it is well posed as an initial value problem. In addition, jump conditions must be uniquely defined. This is not totally obvious due to the presence of first-order non-conservative terms in the closed set of PDEs. Retaining the latter constraints, in order to have a suitable model for the considered flows, we end up with the following specifications for the three-phase flow model:

(i) Shock relations are well defined **(C1)**,

(ii) An entropy inequality holds for smooth solutions of the whole model **(C2)**,

(iii) Fast transients may be computed in a meaningful way **(C3)**.

Actually, as recalled in section 2, the governing set of PDEs first requires a relevant definition of the interfacial velocity $\mathscr{V}_i$, and of interfacial pressures $\Pi_{k,l}$. We briefly recall now the modeling strategy introduced in [25], which is grounded on the one introduced for the two-phase flow framework in [10]. First of all, the following form of the interfacial velocity $\mathscr{V}_i$ is assumed, as a convex combination of phasic velocities U_k:

$$\mathscr{V}_i(W) = \sum_k \beta_k(W) U_k \tag{1}$$

(where W stands for the state variable and the β_k are positive functions that remains to be prescribed), which is a priori meaningful since it is Galilean invariant when: $\sum_k \beta_k(W) = 1$. This form is also expected from a phenomenological point of view. Then, the entropy inequality governing the entropy of the mixture **(C2)** enables to exhibit a **unique set of interfacial pressures** $\Pi_{k,l}$, which only depend on the $\beta_k(W)$ (see appendix G in [25]). This in turn allows to propose a class of admissible source terms $S(W)$ (depending on the local state variable W), in order to comply with the entropy inequality **(C2)**. The latter source terms require physically relevant relaxation time scales, to be found in the two-phase flow literature.

Eventually, it only remains to propose a suitable form of functions $\beta_k(W)$ in order to comply with condition **(C1)**. This is achieved in practice by enforcing the linearly degenerate structure to the field associated with eigenvalue $\lambda = \mathscr{V}_i$. It turns out that, as a result, the third condition **(C3)** will be guaranteed, assuming a weak condition on the parameter $\mathscr{M}_k = \dfrac{U_k - \mathscr{V}_i(W)}{c_k}$, that is:

$$|\mathscr{M}_k| \neq 1. \tag{2}$$

Thus, the paper is organized as follows. The full model , including all closure laws, is first recalled in section 2, together with its main properties. Then, focus is given in section 3 on the true relaxation process associated with source terms. Afterwards, section 4 will detail the numerical approach which relies on a two-step explicit/implicit method, where the convective part of the model is estimated first, using an explicit scheme, while the second step takes all source terms into account in an linear-implicit way. The explicit strategy in step 1 enables to define a time step which in some sense guarantees an optimal accuracy of fast waves. The implicit algorithm proposed in step 2 is derived from the analysis conducted in section 3, and its properties are given. The last section provides results of some numerical experiments, including some numerical study of convergence with respect to the mesh size.

1 The immiscible three-phase flow model [25]

We consider an immiscible, compressible, non-equilibrium, three-phase flow model. In the application section 4, phase 1 will correspond to a liquid metal, phase 2 to liquid water and phase 3 to water vapour. First, as the model is assumed to be immiscible, we have the structural constraint:

$$\alpha_1 + \alpha_2 + \alpha_3 = 1 \ . \tag{3}$$

where $\forall k \in [\![1,3]\!]$, $\alpha_k \in]0,1[$ denote the statistical fractions of each phase. Moreover, since the model is in full disequilibrium, each phase k $\in [\![1,3]\!]$ is given a velocity U_k, a density ρ_k, a partial density $m_k = \alpha_k \rho_k$, a pressure P_k and a specific entropy s_k. The total energies are then defined as:

$$E_k = \rho_k(\epsilon_k(P_k, \rho_k) + U_k^2/2), \tag{4}$$

where $\epsilon_k(P_k, \rho_k)$ denotes the internal energy of each phase k. The internal energy of phase k is bind to pressure P_k and density ρ_k through an Equation of State (EoS). The state variable W writes as:

$$W = (\alpha_2, \alpha_3, m_1, m_1U_1, \alpha_1E_1, m_2, m_2U_2, \alpha_2E_2, m_3, m_3U_3, \alpha_3E_3)^\intercal \ . \tag{5}$$

Then, the model reads (see [25]):

$$\begin{cases} \dfrac{\partial \alpha_k}{\partial t} + \mathscr{V}_I(W)\cdot\nabla\alpha_k = S_k^{\alpha}(W)\ , \\ \dfrac{\partial m_k}{\partial t} + \nabla\cdot(m_k U_k) = S_k^{m}(W)\ , \\ \dfrac{\partial m_k U_k}{\partial t} + \nabla\cdot(m_k U_k\otimes U_k + \alpha_k P_k \mathscr{I}) + \displaystyle\sum_{l=1,l\neq k}^{3}\Pi_{kl}(W)\nabla\alpha_l = S_k^{U}(W)\ , \\ \dfrac{\partial \alpha_k E_k}{\partial t} + \nabla\cdot(\alpha_k U_k(E_k+P_k)) - \displaystyle\sum_{l=1,l\neq k}^{3}\Pi_{kl}(W)\dfrac{\partial\alpha_l}{\partial t} = S_k^{E}(W)\ , \end{cases} \tag{6}$$

where $\mathscr{I}$ is the identity matrix. Moreover, $\mathscr{V}_I$ and Π_{kl} respectively stand for the interfacial velocity and the interfacial pressures. Those interfacial terms, alongside source terms $S_k^{\alpha}(W)$, $S_k^{m}(W)$, $S_k^{U}(W)$ and $S_k^{E}(W)$, have to be specified in order to close the model. To do so, the total entropy $\eta(W)$ paired with its entropy-flux $\mathscr{F}_\eta(W)$, are introduced:

$$\begin{cases} \eta = m_1 s_1(P_1,\rho_1) + m_2 s_2(P_2,\rho_2) + m_3 s_3(P_3,\rho_3)\ , \\ \mathscr{F}_\eta = m_1 U_1 s_1(P_1,\rho_1) + m_2 U_2 s_2(P_2,\rho_2) + m_3 U_3 s_3(P_3,\rho_3)\ . \end{cases} \tag{7}$$

Definitions of the phasic temperature T_k, the phasic Gibbs free energy μ_k, the phasic enthalpy h_k and the phasic celerity c_k are also recalled:

$$\frac{1}{T_k} = \frac{\partial_{P_k}\left(s_k(P_k,\rho_k)\right)|_{\rho_k}}{\partial_{P_k}\left(\epsilon_k(P_k,\rho_k)\right)|_{\rho_k}} \tag{8}$$

$$\mu_k = h_k - T_k S_k \tag{9}$$

$$h_k = \epsilon_k(P_k,\rho_k) + \frac{P_k}{\rho_k} \tag{10}$$

$$c_k^2\ \partial_{P_k}\left(s_k(P_k,\rho_k)\right)|_{\rho_k} + \partial_{\rho_k}\left(s_k(P_k,\rho_k)\right)|_{P_k} = 0 \tag{11}$$

The strategy for closing the model is to ensure that it respects the following mathematical properties: hyperbolicity of the convective part (*i.e.* supposing $S_k^{\alpha} = S_k^{m} = S_k^{U} = S_k^{E} = 0$.), uniqueness of jump relations and compliance to an entropy inequality for the smooth solutions of the model. To do so, we first choose the interfacial velocity $\mathscr{V}_I$ as:

$$\mathscr{V}_I = U_1\ , \tag{12}$$

which leads to the following **unique** interfacial pressure definition, owing to the entropy inequality (see **Appendix** G in [25]):

$$\begin{cases} \Pi_{12} = \Pi_{21} = \Pi_{23} = P_2\ , \\ \Pi_{13} = \Pi_{31} = \Pi_{32} = P_3. \end{cases} \tag{13}$$

Before closing the source terms, let us recall some properties of the convective part of the model in a one dimensional framework.

Reminding that system (6) is invariant under frame rotation, we introduce a unit vector $\vec{n}$ in $\mathbb{R}^3$ and define $x_n = x\cdot n$ n for $k\in[\![1,3]\!]$:

$$w_k = U_k\cdot n \tag{14}$$

$$f_\eta = \mathscr{F}_\eta\cdot n \tag{15}$$

Getting rid of transverse variations and considering null source terms, we end up with the following system in the **one dimensional framework**:

$$\begin{cases} \dfrac{\partial \alpha_k}{\partial t} + w_1\partial_{x_n}\alpha_k = 0\ , \\ \dfrac{\partial m_k}{\partial t} + \partial_{x_n}(m_k w_k) = 0\ , \\ \dfrac{\partial m_k w_k}{\partial t} + \partial_{x_n}(m_k\ w_k^2 + \alpha_k P_k) + \displaystyle\sum_{l=1,l\neq k}^{3}\Pi_{kl}(W)\partial_{x_n}\alpha_l = 0\ , \\ \dfrac{\partial \alpha_k E_k}{\partial t} + \partial_{x_n}\left(\alpha_k w_k(E_k+P_k)\right) - \displaystyle\sum_{l=1,l\neq k}^{3}\Pi_{kl}(W)\dfrac{\partial\alpha_l}{\partial t} = 0\ . \end{cases} \tag{16}$$

Then, according to [25, 26], this sub-system has the following property:

Property 1 *(Convective part of the three-phase flow model in a 1D framework)* :

If $\forall k \in [\![1,3]\!], \alpha_k$ *stay in* $]0,1[$ *and* $|w_k - w_1| \neq c_k$*, then:*

- *System* (16) *is symmetrizable and its associated eigenvalues are:*

$$\begin{array}{l} \lambda_{1,2,3}(W,n) = w_1 \ , \ \lambda_4(W,n) = w_2 \ , \ \lambda_5(W,n) = w_3 \ , \\ \lambda_{6,7}(W,n) = w_1 \pm c_1 \ , \ \lambda_{8,9}(W,n) = w_2 \pm c_2 \ , \ \lambda_{10,11}(W,n) = w_3 \pm c_3 \ . \end{array} \tag{17}$$

- *Fields associated with* λ_k $(k = 6-11)$ *are Genuinely Non Linear (**GNL**). Other fields are Linearly Degenerate (**LD**). Riemann invariants within each wave can be found in [25] **Appendix B** and **Appendix E**.*

- *Jump relations associated with system* (16) *are unique (see [25] **Appendix C**).*

- *Smooth solutions of* (16) *satisfy:*

$$\partial_t \eta + \partial_{x_n} f_\eta = 0 \tag{18}$$

□

Property 1 can be extended to a three-dimensional framework, see [25] and [6].

Then, coming back to the three-dimensional framework and therefore system (6), source terms have to be closed. The strategy for closing those terms is to select a form so that smooth solutions of system (6) comply with the entropy inequality:

$$\partial_t \eta + \nabla \cdot \mathscr{F}_\eta \geqslant 0. \tag{19}$$

We define V_{kl} and H_{kl} as:

$$V_{kl} = \frac{U_k + U_l}{2} \ , \tag{20}$$

$$H_{kl} = \frac{U_k \cdot U_l}{2} \ . \tag{21}$$

It may be checked that the following closure laws for drag effects, mass transfer, heat transfer and pressure relaxation:

$\forall k \in [\![1,3]\!]$:

$$S_k^\alpha = \sum_{l=1,l\neq k}^{3} K_{kl}(W)(P_k - P_l) \quad , \tag{22}$$

$$S_k^m = \sum_{l=1,l\neq k}^{3} \Lambda_{kl}(W) \left(\frac{\mu_l}{T_l} - \frac{\mu_k}{T_k} \right) \quad , \tag{23}$$

$$S_k^U = \sum_{l=1,l\neq k}^{3} d_{kl}(W)(U_l - U_k) + \sum_{l=1,l\neq k}^{3} V_{kl}\Lambda_{kl}(W) \left(\frac{\mu_l}{T_l} - \frac{\mu_k}{T_k} \right) \ , \tag{24}$$

$$S_k^E = \sum_{l=1,l\neq k}^{3} q_{kl}(W)(T_l - T_k) \ + \sum_{l=1,l\neq k}^{3} V_{kl} \cdot (U_l - U_k) d_{kl}(W) + \sum_{l=1,l\neq k}^{3} H_{kl}\Lambda_{kl}(W) \left(\frac{\mu_l}{T_l} - \frac{\mu_k}{T_k} \right), \tag{25}$$

comply with inequality (19). These closures are the straightforward counterpart of two-phase closure laws.

The positive functions $K_{kl}(W)$, $\Lambda_{kl}(W)$, $d_{kl}(W)$ and $q_{kl}(W)$ are defined as:

$$K_{kl}(W) = \frac{\alpha_k \alpha_l}{\mathscr{P}_0 \tau_{kl}^P(W)} \quad , \tag{26}$$

$$\Lambda_{kl}(W) = \frac{m_k m_l}{(m_k + m_l)\Gamma_0 \tau_{kl}^m(W)} \quad , \tag{27}$$

$$d_{kl}(W) = \frac{m_k m_l}{(m_k + m_l)\tau_{kl}^U(W)} \quad , \tag{28}$$

$$q_{kl}(W) = \frac{m_k m_l C_{v_k} C_{v_l}}{(m_k C_{v_k} + m_l C_{v_l})\tau_{kl}^T(W)} \quad . \tag{29}$$

Quantities C_{V_k} denote the specific heat capacities at constant volume. Π_0 is a positive reference pressure, Γ_0 is a positive reference fraction of $\frac{\mu}{T}$.

For each phasic connection $k-l$, $\tau_{kl}^P(W)$, $\tau_{kl}^m(W)$, $\tau_{kl}^T(W)$ and $\tau_{kl}^U(W)$ are the symmetric strictly positive relaxation time scales related to the return to equilibrium of the associated thermodynamic quantity between phase k and l. Closure laws for the relaxation time scales can be found in the two-phase flow literature, see among others [17, 7] for the pressure, [33] for the velocity, [43] for the temperature and [4] for mass transfer.

No assumption about these **strictly** positive time scales is imposed, either when studying the overall relaxation process, or when constructing the numerical scheme for processing the source terms.

The previous closing strategy is detailed in [25] and has been used for other multiphase flow models, see among others [35], [21], [19], [10], [31], [28], [42] for two-phase and three-phase flow models.

We focus in the following section on the expected inner relaxation process.

2 Relaxation process in the model

This part aims at studying the expected inner relaxation process inside the model associated with the source terms (22), (23), (24) and (25). First, as phase 1 is in this paper supposed to be a liquid metal, no phase change with phase 2 (liquid water) and 3 (water vapour) can occur physically, which is equivalent to take:

$$\Lambda_{12}(W) = \Lambda_{13}(W) = 0 \ . \tag{30}$$

For clarity, we set:

$$\forall k \in [\![1,3]\!], \ g_k = \frac{\mu_k}{T_k} \tag{31}$$

Then, we suppose the following:

$$\forall k \in [\![1,3]\!] \ , \ \forall \Psi \in \{\alpha_k, P_k, U_k, m_k U_k, \alpha_k E_k\} \ , \ \nabla \Psi = 0 \ , \tag{32}$$

and we set:

$$\forall (k,l) \in [\![1,3]\!]^2 \ , \ \forall \Phi_k \in \{U_k, P_k, T_k, g_k\} \ , \Delta\Phi_{kl} = \Phi_k - \Phi_l. \tag{33}$$

Then, owing to (32) and (30) system (6) reduces to an ODE system:

$$\left\{ \begin{array}{l} \dfrac{\partial \alpha_k}{\partial t} = \displaystyle\sum_{l=1, l\neq k}^{3} K_{kl}(W)\Delta P_{kl} \ , \\ \dfrac{\partial m_k}{\partial t} = - \displaystyle\sum_{l=1, l\neq k}^{3} \Lambda_{kl}(W)\Delta g_{kl} \ , \\ \dfrac{\partial m_k U_k}{\partial t} = - \displaystyle\sum_{l=1, l\neq k}^{3} d_{kl}(W)\Delta U_{kl} - \displaystyle\sum_{l=1, l\neq k}^{3} V_{kl}\Lambda_{kl}(W)\Delta g_{kl} \ , \\ \dfrac{\partial \alpha_k E_k}{\partial t} - \displaystyle\sum_{l=1, l\neq k}^{3} \Pi_{kl}(W)\dfrac{\partial \alpha_l}{\partial t} = - \displaystyle\sum_{l=1, l\neq k}^{3} q_{kl}(W)\Delta T_{kl} - \displaystyle\sum_{l=1, l\neq k}^{3} V_{kl} d_{kl}(W)\Delta U_{kl} - \displaystyle\sum_{l=1, l\neq k}^{3} H_{kl}\Lambda_{kl}(W)\Delta g_{kl} \ . \end{array} \right. \tag{34}$$

Considering hypothesis (30), and using the definition of V_{kl}, of H_{kl}, of the sound speed c_k and of the Gibbs free energy μ_k, then, for each phase $k \in [\![1,3]\!]$, equations of evolution of velocity U_k, pressure P_k, temperature T_k and fraction g_k can be derived from system (34). Therefore, governing equations of the gaps: $\Delta U_{12}, \Delta U_{13}, \Delta P_{12}, \Delta P_{13}, \Delta T_{12}, \Delta T_{13}, \Delta g_{23}$ can be obtained. Those equations can be rewritten as one equation of evolution of the quantity:

$$\Delta^r = (\Delta U_{12}, \Delta U_{13}, \Delta P_{12}, \Delta P_{13}, \Delta T_{12}, \Delta T_{13}, \Delta g_{23})^\intercal \in \mathbb{R}^7 . \tag{35}$$

The equation of evolution associated with Δ^r reads as:

$$\partial_t (\Delta^r) = -\mathscr{R}^{relax}(W)\Delta^r , \tag{36}$$

where the non symmetric matrix $\mathscr{R}^{relax}$ in $\mathscr{M}_7(\mathbb{R})$ takes the form:

$$\mathscr{R}^{relax} = \begin{pmatrix} R_{UU} & 0 \\ R_U & \mathscr{R}_{thermo} \end{pmatrix} , \tag{37}$$

where $R_{UU} \in \mathscr{M}_2(\mathbb{R})$, $\mathscr{R}_{thermo} \in \mathscr{M}_5(\mathbb{R})$ and $R_U \in \mathscr{M}_{5,2}(\mathbb{R})$.

All coefficients of $\mathscr{R}^{relax}$ can be found in **Appendix 2**.

The velocity relaxation process has a peculiar role in the global relaxation process. A similar result has been found in the framework of a two-phase flow model, see [29].

Alongside equation (36), when considering hypothesis (30) and (32), the following conservation laws can be deduced from system (34):

$$\partial_t (m_1) = 0 \tag{38}$$
$$\partial_t (m_2 + m_3) = 0 \tag{39}$$
$$\partial_t (m_1 U_1 + m_2 U_2 + m_3 U_3) = 0 \tag{40}$$
$$\partial_t (\alpha_1 E_1 + \alpha_2 E_2 + \alpha_3 E_3) = 0 \tag{41}$$

Hence, we have four stationary constraints (38), (39), (40), (41), plus seven unsteady equations embedded in (36).

From equation (36), effective relaxation conditions can be obtained for model (6).

Property 2 *(Necessary conditions for effective relaxation of the three-phase flow model):*

- *The velocity relaxation process occurs when:*

$$tr(R_{UU}) > 0 , \tag{42}$$
$$det(R_{UU}) > 0 . \tag{43}$$

- *We note, for $i \in [\![1,5]\!]$, λ_i the real or complex conjugate eigenvalues of $\mathscr{R}_{thermo}$. If the thermodynamic relaxation process is effective, then we have:*

$$\Sigma_1 = tr(\mathscr{R}_{thermo}) > 0 , \tag{44}$$
$$\Sigma_2 = \sum_{i<j} \lambda_i \lambda_j > 0 , \tag{45}$$
$$\Sigma_3 = \sum_{i<j<k} \lambda_i \lambda_j \lambda_k > 0 , \tag{46}$$
$$\Sigma_4 = \sum_{i<j<k<l} \lambda_i \lambda_j \lambda_k \lambda_l > 0 , \tag{47}$$
$$\Sigma_5 = det(\mathscr{R}_{thermo}) > 0 , \tag{48}$$

□

Proof. The proof reads as follows:

- First item of **Property 2**:

  i) if the velocity relaxation occurs, then the real parts of the two eigenvalues l_1 and l_2 of matrix R_{UU} are strictly positive. Then, the two conditions (42) and (43) are easily verified.

  ii) Moreover, if conditions (42) and (43) are verified, it is trivial that both real parts of l_1 and l_2 are positive.

  Besides, if mass transfer between phase 2 and 3 is neglected, *i.e.* $\Lambda_{23} = 0$, conditions (42) and (43) always stand true, since $d_{kl} > 0$ and $tr(R_{UU})$ and $det(R_{UU})$ read:

$$tr(R_{UU}) = \frac{1}{m_1}(d_{12} + d_{13}) + \frac{1}{m_2}(d_{12} + d_{23}) + \frac{1}{m_3}(d_{13} + d_{23}) > 0$$
$$det(R_{UU}) = \left[\frac{1}{m_1 m_2} + \frac{1}{m_1 m_3} + \frac{1}{m_2 m_3}\right](d_{12}d_{13} + d_{12}d_{23} + d_{13}d_{23}) > 0$$

- If the thermodynamic relaxation process is effective, then the real part of the five eigenvalues of $\mathscr{R}_{thermo}$, $\lambda_i,\ i \in [\![1,5]\!]$ is positive. The five coefficients Σ_1, Σ_2, Σ_3, Σ_4 and Σ_5 write:

$$\Sigma_1 = \lambda_1 + \lambda_2 + \lambda_3 + \lambda_4 + \lambda_5 \ ,$$
$$\Sigma_2 = \lambda_1\lambda_2 + \lambda_1\lambda_3 + \lambda_1\lambda_4 + \lambda_1\lambda_5 + \lambda_2\lambda_3 + \lambda_2\lambda_4 + \lambda_2\lambda_5 + \lambda_3\lambda_4 + \lambda_3\lambda_5 + \lambda_4\lambda_5 \ ,$$
$$\Sigma_3 = \lambda_1\lambda_2\lambda_3 + \lambda_1\lambda_2\lambda_4 + \lambda_1\lambda_2\lambda_5 + \lambda_1\lambda_3\lambda_4 + \lambda_1\lambda_3\lambda_5 + \lambda_1\lambda_4\lambda_5 + \lambda_2\lambda_3\lambda_4 + \lambda_2\lambda_3\lambda_5 + \lambda_2\lambda_4\lambda_5 + \lambda_3\lambda_4\lambda_5 \ ,$$
$$\Sigma_4 = \lambda_2\lambda_3\lambda_4\lambda_5 + \lambda_1\lambda_3\lambda_4\lambda_5 + \lambda_1\lambda_2\lambda_4\lambda_5 + \lambda_1\lambda_2\lambda_3\lambda_5 + \lambda_1\lambda_2\lambda_3\lambda_4 \ ,$$
$$\Sigma_5 = \lambda_1\lambda_2\lambda_3\lambda_4\lambda_5 \ .$$

  As $\mathscr{R}_{thermo}$ lies in $\mathscr{M}_5(\mathbb{R})$, three cases can occur:

Case 1: All of the eigenvalues of $\mathscr{R}_{thermo}$ are real. Then, if all eigenvalues of $\mathscr{R}_{thermo}$ are positive, all coefficients $\Sigma_n,\ n \in [\![1,5]\!]$ are trivially positive.

Case 2: One eigenvalue of $\mathscr{R}_{thermo}$ is real (let's call it λ_1) and the other four are complex and form two pairs of complex conjugate ($\lambda_3 = \overline{\lambda_2}$ and $\lambda_5 = \overline{\lambda_4}$). Thus, coefficients $\Sigma_n,\ n \in [\![1,5]\!]$ write as:

$$\Sigma_1 = \lambda_1 + 2\mathfrak{Re}(\lambda_2) + 2\mathfrak{Re}(\lambda_4) \ , \tag{49}$$
$$\Sigma_2 = 2\lambda_1\mathfrak{Re}(\lambda_2) + 2\lambda_1\mathfrak{Re}(\lambda_4) + 4\mathfrak{Re}(\lambda_2)\mathfrak{Re}(\lambda_4) + |\lambda_2|^2 + |\lambda_4|^2 \ , \tag{50}$$
$$\Sigma_3 = \lambda_1\left(|\lambda_2|^2 + |\lambda_4|^2\right) + 4\lambda_1\mathfrak{Re}(\lambda_2)\mathfrak{Re}(\lambda_4) + 2|\lambda_2|^2\mathfrak{Re}(\lambda_4) + 2|\lambda_4|^2\mathfrak{Re}(\lambda_2) \ , \tag{51}$$
$$\Sigma_4 = 2\lambda_1\left(\mathfrak{Re}(\lambda_4)|\lambda_2|^2 + \mathfrak{Re}(\lambda_2)|\lambda_4|^2\right) + |\lambda_2|^2|\lambda_4|^2 \ , \tag{52}$$
$$\Sigma_5 = \lambda_1|\lambda_2|^2|\lambda_4|^2 \ . \tag{53}$$

  If all the real parts of the eigenvalues of $\mathscr{R}_{thermo}$ are strictly positive, one can easily check from the previous notations that:

$$\forall n \in [\![1,5]\!], \Sigma_n > 0 \tag{54}$$

Case 3: Three eigenvalues of $\mathscr{R}_{thermo}$ are real: λ_1, λ_2 and λ_3. The remaining two are complex conjugate $\lambda_5 = \overline{\lambda_4}$. Thus, coefficients $\Sigma_n,\ n \in [\![1,5]\!]$ write:

$$\Sigma_1 = \lambda_1 + \lambda_2 + \lambda_3 + 2\mathfrak{Re}(\lambda_4) \ , \tag{55}$$
$$\Sigma_2 = (\lambda_1\lambda_2 + \lambda_1\lambda_3 + \lambda_2\lambda_3) + 2(\lambda_1 + \lambda_2 + \lambda_3)\mathfrak{Re}(\lambda_4) + |\lambda_4|^2 \ , \tag{56}$$
$$\Sigma_3 = \lambda_1\lambda_2\lambda_3 + 2(\lambda_1\lambda_2 + \lambda_1\lambda_3 + \lambda_2\lambda_3)\mathfrak{Re}(\lambda_4) + (\lambda_1 + \lambda_2 + \lambda_3)|\lambda_4|^2 \ , \tag{57}$$
$$\Sigma_4 = 2\lambda_1\lambda_2\lambda_3\mathfrak{Re}(\lambda_4) + (\lambda_1\lambda_2 + \lambda_1\lambda_3 + \lambda_2\lambda_3)|\lambda_4|^2 \ , \tag{58}$$
$$\Sigma_5 = \lambda_1\lambda_2\lambda_3|\lambda_4|^2 \ . \tag{59}$$

  If all the real parts of the eigenvalues of $\mathscr{R}_{thermo}$ are strictly positive, we can once again easily check from the previous notations that:

$$\forall n \in [\![1,5]\!], \Sigma_n > 0 \tag{60}$$

□

Remark 2:

i) Necessary conditions of effective relaxation (44), (45), (46), (47), (48) cannot be proved to always stand true for any EoS. They have therefore to be numerically tested. The counterpart of **Property 2** has been exhibited in the framework of an immiscible two-phase flow model in [29]. In the latter reference, a detailed analysis of relaxation conditions is added when restricting to a mixture of stiffened gases EoS.

ii) The inner relaxation process has also been studied in [30], considering the hybrid two-phase flow model [31].

3 Numerical scheme

This parts aims at building a numerical strategy for computing approximate solutions of system (6). The overall strategy is close to the one detailed in [6]. However, the scheme proposed in the sequel differs in its treatment of the source terms.

First, let's recall the global numerical approach presented in [6] for the current model, but also used in [27, 12], among others, for a two-phase flow framework. This strategy consists in two steps:

- Compute an approximate solution of the following subsystem associated with the convective part of the model:

$$\begin{cases} \dfrac{\partial \alpha_k}{\partial t} + \mathscr{V}_I(W)\cdot\nabla\alpha_k = 0 \ , \\ \dfrac{\partial m_k}{\partial t} + \nabla\cdot(m_k U_k) = 0 \ , \\ \dfrac{\partial m_k U_k}{\partial t} + \nabla\cdot(m_k U_k\otimes U_k + \alpha_k P_k \mathscr{I}) + \displaystyle\sum_{l=1,l\neq k}^{3} \Pi_{kl}(W)\nabla\alpha_l = 0 \ , \\ \dfrac{\partial \alpha_k E_k}{\partial t} + \nabla\cdot(\alpha_k E_k U_k + \alpha_k P_k U_k) - \displaystyle\sum_{l=1,l\neq k}^{3} \Pi_{kl}(W)\dfrac{\partial \alpha_l}{\partial t} = 0 \ , \end{cases} \tag{61}$$

  using an **explicit** Riemman solver adapted for non-conservative products. This first step fully determines the time step Δt. Details of this step can be found in [6].

- Then, solve with a **linear-implicit** scheme on a time step Δt, the stiff system (34). It is the counterpart of (6) without the convective terms. In [6], this step is conducted with a fractional step approach, which decouples all relaxation effects for velocity, pressure, temperature, Gibbs free energy. The new approach proposed here follows the same strategy as the one in [29] in the framework of an immiscible two-phase flow model [1].

To begin with, as in [29], we take advantage of the block triangular structure of $\mathscr{R}^{relax}$. Indeed, as the velocity relaxation is less coupled with the other relaxation effects, we choose to treat it beforehand with the same method as the one presented in [6] and recalled in **Appendix 3**.

In the sequel, in order to ease notations, the instant right after the velocity relaxation will be referred as t^n.

Then, (34) becomes:

$$\begin{cases} \dfrac{\partial \alpha_k}{\partial t} = \displaystyle\sum_{l=1,l\neq k}^{3} K_{kl}(W)\Delta P_{kl} \ , \\ \dfrac{\partial m_k}{\partial t} = -\displaystyle\sum_{l=1,l\neq k}^{3} \Lambda_{kl}(W)\Delta g_{kl} \ , \\ \dfrac{\partial m_k U_k}{\partial t} = -\displaystyle\sum_{l=1,l\neq k}^{3} V_{kl}\Lambda_{kl}(W)\Delta g_{kl} \ , \\ \dfrac{\partial \alpha_k E_k}{\partial t} - \displaystyle\sum_{l=1,l\neq k}^{3} \Pi_{kl}(W)\dfrac{\partial \alpha_l}{\partial t} = -\displaystyle\sum_{l=1,l\neq k}^{3} q_{kl}(W)\Delta T_{kl} - \sum_{l=1,l\neq k}^{3} H_{kl}\Lambda_{kl}(W)\Delta g_{kl} \ . \end{cases} \tag{62}$$

We also have the conservation law of the sum of the total energies:

$$\partial_t \sum_{k=1}^{3} \alpha_k E_k = 0 \tag{63}$$

From system (62), one can obtain:

$$m_k \partial_t \left(\frac{U_k^2}{2} \right) = -U_k \sum_{l \neq k} \left(V_{kl} - U_k \right) \Lambda_{kl}(W) \Delta g_{kl} \ . \tag{64}$$

Thus, using (20), we have:

$$\partial_t \left(\frac{1}{2} m_k U_k^2 \right) = - \sum_{l \neq k} H_{kl} \Lambda_{kl}(W) \Delta g_{kl} \ . \tag{65}$$

Therefore, from (62), we get:

$$\partial_t \left(m_k \epsilon_k \right) - \sum_{l=1, l \neq k}^{3} \Pi_{kl}(W) \frac{\partial \alpha_l}{\partial t} = - \sum_{l=1, l \neq k}^{3} q_{kl}(W) \Delta T_{kl} \ . \tag{66}$$

Then, a conservation law for the sum of the internal energies ϵ_k weighted by the partial densities m_k can be deduced and reads:

$$\partial_t \left(\sum_{k=1}^{3} m_k \epsilon_k \right) = 0 \ . \tag{67}$$

We also recall that the immiscible constraint (3) always stands true and can be seen as a stationary constraint:

$$\partial_t \left(\alpha_1 + \alpha_2 + \alpha_3 \right) = 0 \ . \tag{68}$$

Next, as in the previous part, an evolution equation of the quantity:

$$\Delta_{thermo} = \left(\Delta P_{12}, \Delta P_{13}, \Delta T_{12}, \Delta T_{13}, \Delta g_{23} \right)^{\intercal} \ , \tag{69}$$

is constructed from (62):

$$\partial_t \left(\Delta_{thermo} \right) = -\mathscr{R}_{thermo} \Delta_{thermo} \ , \tag{70}$$

where $\mathscr{R}_{thermo}$ is the sub-matrix of $\mathscr{R}^{relax} \in \ \mathscr{M}_5(\mathbb{R})$ arising in (37). We recall that coefficients of matrix $\mathscr{R}^{relax}$ are given in **Appendix 2**. Alongside (70) and still considering (67) and (3), the following can also be obtained from (62):

$$\partial_t \left(m_1 \right) = 0 \tag{71}$$

$$\partial_t \left(m_2 + m_3 \right) = 0 \tag{72}$$

$$\partial_t \left(m_1 U_1 \right) = 0 \tag{73}$$

$$\partial_t \left(m_2 U_2 + m_3 U_3 \right) = 0 \tag{74}$$

To summarize, we end up with eleven unknowns, six steady constraints (63), (67), (71), (72), (73), (74) and the set of ODEs (70) Eventually, the new algorithm writes as:

Algorithm: *(Coupled P-T-g algorithm)*

Step 1: Estimate the evolution of Δ_{thermo} through (70) by using an Euler implicit scheme with $\mathscr{R}_{thermo}$ frozen at time t^n:

$$\Delta_{thermo}^{n+1} = \left(\mathscr{I} + \Delta t \mathscr{R}_{thermo}^{n} \right)^{-1} \Delta_{thermo}^{n}. \tag{75}$$

Step 2: Setting: $\tilde{M}_n = m_2^n + m_3^n$, compute the partial densities at time t^{n+1}:

$$\begin{cases} m_1^{n+1} = m_1^n \\ m_2^{n+1} = \dfrac{\tilde{M}_n}{1 + \frac{(\tilde{M}_n - m_2^n)}{m_2^n} \exp\left(\frac{\Delta g_{23}^{n+1}}{\tau_{23}^{m^n} \Gamma_0} \Delta t \right)} > 0 \\ m_3^{n+1} = \tilde{M}_n - m_2^{n+1} \end{cases} \tag{76}$$

Thus complying with the steady constraints (71), (72).

Step 3: Write:

$$P_2^{n+1} = P_1^{n+1} - \Delta P_{12}^{n+1} \ , \tag{77}$$
$$P_3^{n+1} = P_1^{n+1} - \Delta P_{13}^{n+1} \ , \tag{78}$$
$$T_2^{n+1} = T_1^{n+1} - \Delta T_{12}^{n+1} \ , \tag{79}$$
$$T_3^{n+1} = T_1^{n+1} - \Delta T_{13}^{n+1} \ , \tag{80}$$
$$\tag{81}$$

and note, with help of (67):

$$\xi_n := \sum_{k=1}^{3} (m_k \epsilon_k)^n = \sum_{k=1}^{3} (m_k \epsilon_k)^{n+1}. \tag{82}$$

Then, find P_1^{n+1} and T_1^{n+1} in the admissible range, solutions of the implicit **non-linear** system composed of the discrete counterpart of (67):

$$m_1^{n+1}\epsilon_1(P_1^{n+1}, T_1^{n+1}) + m_2^{n+1}\epsilon_2(P_2^{n+1}, T_2^{n+1}) + m_3^{n+1}\epsilon_3(P_3^{n+1}, T_3^{n+1}) = \xi_n \ , \tag{83}$$

and the discrete counterpart of (3):

$$\frac{m_1^{n+1}}{\rho_1(P_1^{n+1}, T_1^{n+1})} + \frac{m_2^{n+1}}{\rho_2(P_2^{n+1}, T_2^{n+1})} + \frac{m_3^{n+1}}{\rho_3(P_3^{n+1}, T_3^{n+1})} = 1 \ . \tag{84}$$

Step 4: Update local variables P_2^{n+1}, P_3^{n+1}, T_2^{n+1}, T_3^{n+1}, α_1^{n+1}, α_2^{n+1}, α_3^{n+1}:

$$P_2^{n+1} = P_1^{n+1} - \Delta P_{12}^{n+1} \ , \tag{85}$$
$$P_3^{n+1} = P_1^{n+1} - \Delta P_{13}^{n+1} \ , \tag{86}$$
$$T_2^{n+1} = T_1^{n+1} - \Delta T_{12}^{n+1} \ , \tag{87}$$
$$T_3^{n+1} = T_1^{n+1} - \Delta T_{13}^{n+1} \ , \tag{88}$$
$$\alpha_1^{n+1} = \frac{m_1^{n+1}}{\rho_1(P_1^{n+1}, T_1^{n+1})} \ , \tag{89}$$
$$\alpha_2^{n+1} = \frac{m_2^{n+1}}{\rho_2(P_2^{n+1}, T_2^{n+1})} \ , \tag{90}$$
$$\alpha_3^{n+1} = 1 - \alpha_1^{n+1} - \alpha_2^{n+1} = \frac{m_3^{n+1}}{\rho_3(P_3^{n+1}, T_3^{n+1})} \ . \tag{91}$$

Step 5: Then, setting: $\Gamma_{23} = \Lambda_{23}\Delta g_{23}$, compute U_2^{n+1} and U_3^{n+1} solutions of:

$$\begin{cases} (m_2U_2)^{n+1} - (m_2U_2)^n = \Delta t \dfrac{\Gamma_{23}^{n+1}}{2}(U_2^{n+1} + U_3^{n+1}) \ , \\ (m_3U_3)^{n+1} - (m_3U_3)^n = -\Delta t \dfrac{\Gamma_{23}^{n+1}}{2}(U_2^{n+1} + U_3^{n+1}) \ , \end{cases} \tag{92}$$

Step 6: Update the total energies as:

$$\begin{cases} (\alpha_2 E_2)^{n+1} = m_2^{n+1}\epsilon_2(P_2^{n+1}, T_2^{n+1}) + \dfrac{1}{2}m_2^{n+1}(U_2^{n+1})^2 \ , \\ (\alpha_3 E_3)^{n+1} = m_3^{n+1}\epsilon_3(P_3^{n+1}, T_3^{n+1}) + \dfrac{1}{2}m_3^{n+1}(U_3^{n+1})^2 \ , \\ (\alpha_1 E_1)^{n+1} = (\alpha_1 E_1)^n + (\alpha_2 E_2)^n + (\alpha_3 E_3)^n - (\alpha_2 E_2)^{n+1} - (\alpha_3 E_3)^{n+1} \ , \end{cases} \tag{93}$$

using conservation law (63).

□

Property 3 *(The Coupled P-T-g algorithm):*

- *If the discrete relaxation process is effective over time, then the principal minors* Σ_i *,* $i \in [\![1,5]\!]$ *of matrix* $\mathscr{R}_{thermo}$ *are positive at each instant and at every point.*
- *For a mixture of three perfect gas (EoS), solutions of* (83) *and* (84) *exist and are unique inside their definition domain. Moreover,* (84) *ensures that, for* $k \in [\![1,3]\!]$*,* α_k *stays in* $]0,1[$*.*

□

The proof is similar to the one given in [29]. We briefly recall the main guidelines:

Proof.

- The first item is the discrete counterpart of **Property 2**. Indeed, if the thermodynamic relaxation is effective at time t^n, then the real parts of the eigenvalues of $\mathscr{R}^n_{thermo}$ are positive and therefore, (75) ensures a contraction of Δ_{thermo}.
- Consider a mixture of three perfect gases, $k \in \{1,3\}$:

$$P_k = \rho_k(\gamma_k - 1)\epsilon_k \ , \tag{94}$$
$$C_{v_k} T_k = \epsilon_k \ . \tag{95}$$

  Thus equation (83) degenerates into:

$$m_1^{n+1} C_{v_1} T_1^{n+1} + m_2^{n+1} C_{v_2}(T_1^{n+1} - \Delta T_{12}^{n+1}) + m_3^{n+1} C_{v_2}(T_1^{n+1} - \Delta T_{13}^{n+1}) = \xi_n \ , \tag{96}$$

  which can be solved directly and gives a positive T_1^{n+1}.

  Then, a classical function analysis of (84) shows that there exists a unique solution of P_1^{n+1} which lays inside its definition domain.

□

Remark: The first item of **Property 3** can be seen as a way to numerically check if the relaxation process is effective or not in a test case at any time and everywhere. Indeed, coefficients Σ_i, for $i \in [\![1,5]\!]$ correspond to the coefficients of the characteristic polynomial of $\mathscr{R}_{thermo}$:

$$P_5(\lambda) = \lambda^5 - \Sigma_1\lambda^4 + \Sigma_2\lambda^3 - \Sigma_3\lambda^2 + \Sigma_4\lambda - \Sigma_5 \ , \tag{97}$$

and thus can be identified to the principal minors of $\mathscr{R}_{thermo}$. Those quantities Σ_i $i \in [\![1,5]\!]$ can be calculated directly from $\mathscr{R}_{thermo}$. In practice, we use *Maxima* [37], a computer algebra system to compute Σ_i , $i \in [\![1,5]\!]$.

4 Numerical Results:

This part can be broken down into two main subsections. The first one aims at testing only the new algorithm presented above for treating the thermodynamic part of the source terms. On the other hand, the second part is dedicated at confronting the new algorithm, coupled with the velocity relaxation algorithm recalled in **Appendix 3**, and the convective solver taken from [6], to an experimental test case of vapour explosion called KROTOS 44 [32]. Numerical results of this test case will also be compared to [6], where a similar numerical simulation is conducted.

4.1 The homogeneous case

In this subsection, we consider a flow, such that:

$$\forall k \in [\![1,3]\!], U_k = 0 \ , \tag{98}$$
$$\forall k \in [\![1,3]\!], \ \forall \Psi_k \in \{\alpha_k, P_k, T_k, \alpha_k E_k\}, \ \nabla\Psi = 0. \tag{99}$$

It corresponds to a zero-dimensional flow where only the thermodynamic relaxation process takes place.

Then we choose:

$$\begin{cases} \mathscr{P}_0 = \alpha_1^0\alpha_2^0\left(\dfrac{\rho_1^0(c_1^0)^2}{\alpha_1^0}+\dfrac{\rho_2^0(c_2^0)^2}{\alpha_2^0}\right)+\alpha_1^0\alpha_3^0\left(\dfrac{\rho_1^0(c_1^0)^2}{\alpha_1^0}+\dfrac{\rho_3^0(c_3^0)^2}{\alpha_3^0}\right)+\alpha_2^0\alpha_3^0\left(\dfrac{\rho_2^0(c_2^0)^2}{\alpha_2^0}+\dfrac{\rho_3^0(c_3^0)^2}{\alpha_3^0}\right) \\ \Gamma_0 = \left| m_3^0(\gamma_2 C_{v_2}+\dfrac{\epsilon_{2_0}}{T_2^0}(2+\dfrac{\epsilon_{2_0}}{C_{v_2}T_2^0}))+m_2^0(\gamma_3 C_{v_3}+\dfrac{\epsilon_{3_0}}{T_3^0}(2+\dfrac{\epsilon_{3_0}}{C_{v_3}T_3^0}))\right| \end{cases} \tag{100}$$

All relaxation time scales are supposed to be constant in this sub-section. Moreover, they are taken to be equal on each phasic link:

$$\forall \Psi \in P,T : \tau_{12}^{\Psi} = \tau_{13}^{\Psi} = \tau_{23}^{\Psi} = \tau^{\Psi} \ , \tag{101}$$

and

$$\tau_{23}^{m} = \tau^{m}. \tag{102}$$

Their values, the EoS coefficients within each phase and the initial conditions are given in **Appendix** 1. Two test cases are computed. The only differences between case A and case B are the values of the relaxation time scales.

Figures 1, 2, 3 and 4 show that the effective relaxation time scale of the global system is significantly larger than the biggest relaxation time scale among τ^P, τ^T, τ^m, which is 10^{-2}s here. A similar behaviour has already been pointed out for a two-phase flow model in [29] and a detailed analysis is proposed in **Appendix A** of [34] for a two-phase flow model without mass transfer. Moreover, even for a coarse time step, the method captures rather well the behaviour of the solution for both cases. **Figures** 1 and 3 show the impact of the choice of the pressure relaxation time scale on the behaviour of the solution. Up to the author, it advocates to avoid making strong assumptions on the relaxation time scales, when aiming at a fair representation of the transient regime. We emphasize that test case A cannot be computed using the fractional step algorithm presented in [6].

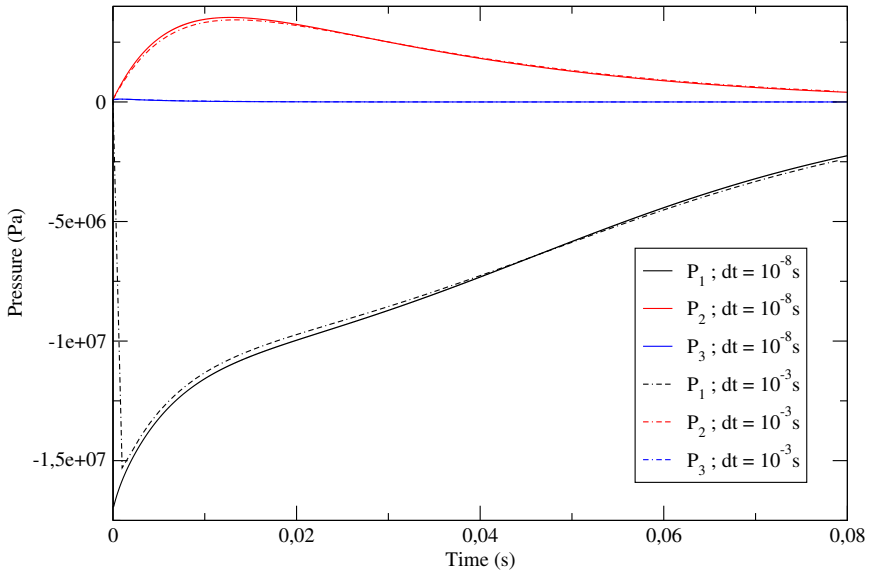

Figure 1: Pressure evolution for **case A** ($\tau^P = 10^{-5}s$, $\tau^T = 10^{-3}s$ and $\tau^m = 10^{-2}s$) computed with two different time stepping: $\Delta t = 10^{-8}s$ and $\Delta t = 10^{-3}s$ (dashed lines).

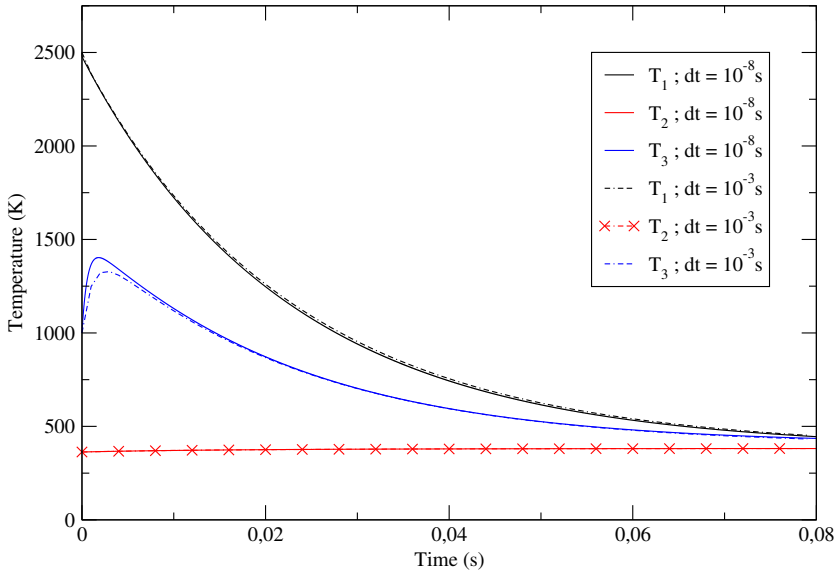

Figure 2: Temperature evolution for **case** A ($\tau^P = 10^{-5}s$, $\tau^T = 10^{-3}s$ and $\tau^m = 10^{-2}s$) computed with two different time stepping: $\Delta t = 10^{-8}s$ and $\Delta t = 10^{-3}s$ (dashed lines).

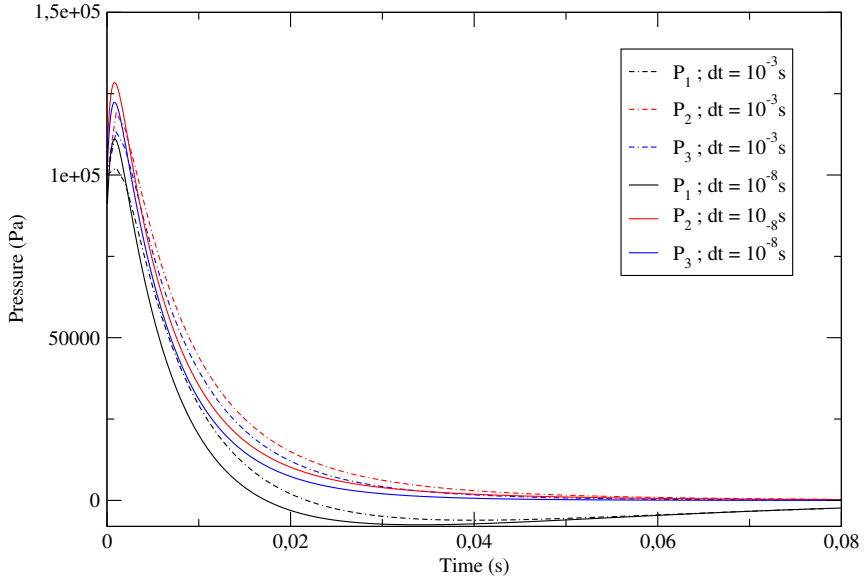

Figure 3: Pressure evolution for **case B** ($\tau^P = 10^{-8}s$, $\tau^T = 10^{-3}s$ and $\tau^m = 10^{-2}s$) computed with two different time stepping: $\Delta t = 10^{-8}s$ and $\Delta t = 10^{-3}s$ (dashed lines).

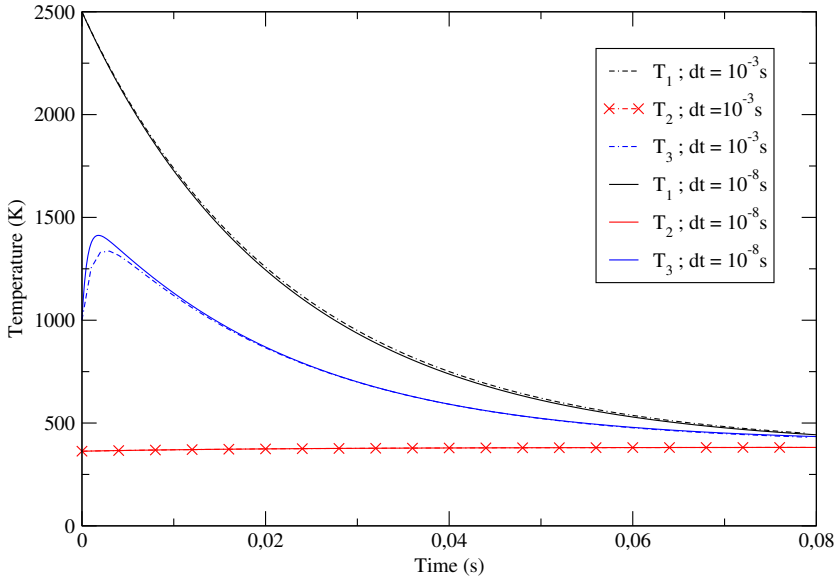

Figure 4: Temperature evolution for **case B** ($\tau^P = 10^{-8}s$, $\tau^T = 10^{-3}s$ and $\tau^m = 10^{-2}s$) computed with two different time stepping: $\Delta t = 10^{-8}s$ and $\Delta t = 10^{-3}s$ (dashed lines).

Eventually, a convergence test is presented in Figure 5. As no analytical solution of system (62) can be exhibited, the solution is compared to a refined computation, with a time step $dt_{cv} = 10^{-10}s$ for a

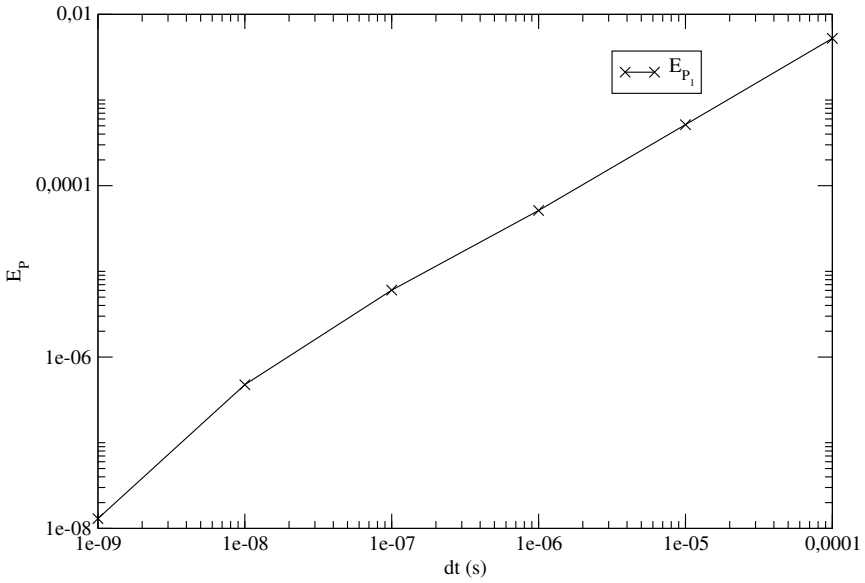

Figure 5: Convergence curve on the pressure P_1 in **case A**.

simulation of $10s$. The error of a quantity κ, $E_\kappa(dt, t = t_{transient})$ is thus defined as:

$$E_\kappa(dt, t = t_{transient}) = \frac{|\kappa_{dt}(t = t_{transient}) - \kappa_{dt_{cv}}(t = t_{transient})|}{\kappa_{dt_{cv}}(t = t_{transient})}, \tag{103}$$

with $\kappa_{dt}(t = t_{transient})$ the value of κ at time $t = t_{transient}$ computed with the numerical scheme presented in section 3 using a time step dt. Figure 5 shows that a convergence rate close to 1 is retrieved.

4.2 Application to KROTOS 44 set up [32]

This section aims at simulating a KROTOS 44 type set up. The set up consists in a one dimension shock tube in water where droplets of liquid corium (phase 1) interact with liquid water (phase 2) and water vapour (phase 3), as shown in **Figure** 6.

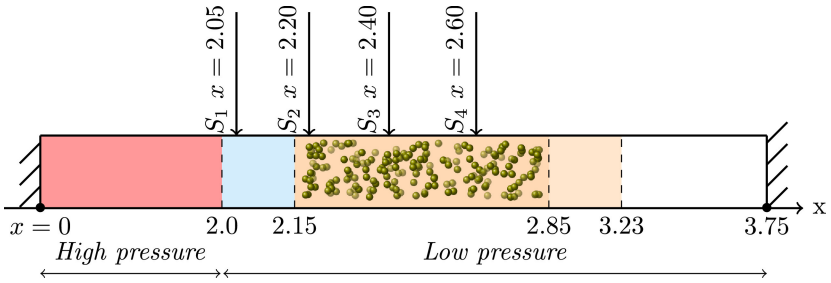

Figure 6: Scheme of the KROTOS-like shock tube

First, at time $t = 0$, velocities are supposed to be null:

$$\forall x \in [0.0, 3.75],\ \forall k \in [\![1, 3]\!],\ U_k(x, t = 0) = 0 \tag{104}$$

Moreover, at time $t = 0$, pressures are initialized in the *high pressure* chamber, see (6), as:

$$\forall x \in [0.0, 2.0],\ \forall k \in [\![1, 3]\!],\ P_k(x, t = 0) = 150\ bar \tag{105}$$

whereas in the *low pressure* chamber, they are set as:

$$\forall x \in [2.0, 3.75],\ \forall k \in [\![1, 3]\!],\ P_k(x, t = 0) = 1\ bar \tag{106}$$

Introducing $\epsilon_{lim} = 10^{-6}$, the initial conditions read:

Abscissa interval (m)	α_2	α_3	T_1 (K)	T_2 (K)	T_3 (K)
High pressure: $x \in [0.0, 2.0]$	$1 - 2\epsilon_{lim}$	ϵ_{lim}	1000	1000	1000
Pure liquid: $x \in]2.0, 2.15]$	$1 - 2\epsilon_{lim}$	ϵ_{lim}	363	363	363
Interaction: $x \in]2.15, 2.85]$	0.884	0.09	2500	363	1000
Plug: $x \in]2.85, 3.23]$	0.835 - ϵ_{lim}	0.165	363	363	363
Cover gas: $x \in]3.23, 3.75]$	ϵ_{lim}	$1 - 2\epsilon_{lim}$	363	363	700

Besides, four numerical probes are set up:

- S_1 is placed at the beginning of the *pure liquid* zone: $x = 2.05m$,
- S_2 is located at the beginning of the *interaction* zone: $x = 2.20m$,
- S_3 is situated at one third of the *interaction* zone: $x = 2.40m$,
- S_4 is positioned at two third of the *interaction* zone: $x = 2.60m$.

Before going further on, as in [29], we need to introduce an evolution equation of the interfacial area $\mathscr{A}_1$ for liquid corium droplets:

$$\mathscr{A}_1 = \frac{6\alpha_1}{D_1} \tag{107}$$

where D_1 stands for the diameter of the corium droplets, which is initialized along the tube at time $t = 0$ as: $D_1 = 15mm$. Indeed, as shown physically in [20] and numerically in [9, 6, 29], taking into account droplet atomization is crucial in order to predict well the energy transfer between phases and therefore to have numerical solutions close to the experimental data. The equation of evolution of the interfacial area (see **Appendix 4**) and its numerical treatment are taken from [5].

We now need to specify for $(k,l) \in [\![1,3]\!]$, $l > k$ the form of the relaxation time scales τ_{kl}^U, τ_{kl}^P, τ_{kl}^T and τ_{kl}^m. On each phasic connection, their form is:

- Velocity relaxation time scales:

$$\frac{1}{\tau_{12}^U} = \frac{1}{\tau_{21}^U} = \frac{0.75 C_d (m_1 + m_2)\|U_1 - U_2\|}{\rho_1 D_1} \; ; \tag{108}$$

$$\frac{1}{\tau_{13}^U} = \frac{1}{\tau_{31}^U} = \frac{0.75 C_d (m_1 + m_3)\|U_1 - U_3\|}{\rho_1 D_1} \; ; \tag{109}$$

$$\frac{1}{\tau_{23}^U} = \frac{1}{\tau_{32}^U} = \frac{0.75 C_d (m_2 + m_3)\|U_2 - U_3\|}{\rho_3 D_3} \; . \tag{110}$$

  This expression of τ_{kl}^U is derived from the Stokes formula [33]. $C_{d_kl} = 24/Re_{kl}$ is the drag coefficient. The Reynolds number Re_{kl} is defined as:

$$Re_{12} = \frac{\rho_2 D_1 \|U_1 - U_2\|}{\mu_2} \tag{111}$$

$$Re_{13} = \frac{\rho_3 D_1 \|U_1 - U_3\|}{\mu_3} \tag{112}$$

$$Re_{23} = \frac{\rho_2 D_3 \|U_2 - U_3\|}{\mu_2} \tag{113}$$

  D_1 and D_3 are the diameter of the corium droplets and the vapour droplets respectively. The corium one is obtained through an interfacial area equation whereas the liquid vapour one is supposed constant: $D_3 = 15mm$.

- Pressure relaxation time scales:

$$\frac{1}{\mathscr{P}_0 \tau_{12}^P} = \frac{1}{\mathscr{P}_0 \tau_{21}^P} = \frac{3}{4\pi\mu_2} \; ; \tag{114}$$

$$\frac{1}{\mathscr{P}_0 \tau_{13}^P} = \frac{1}{\mathscr{P}_0 \tau_{31}^P} = \frac{3}{4\pi\mu_3} \; ; \tag{115}$$

$$\frac{1}{\mathscr{P}_0 \tau_{23}^P} = \frac{1}{\mathscr{P}_0 \tau_{32}^P} = \frac{3}{4\pi\mu_2} \; . \tag{116}$$

$$\tag{117}$$

  where $\mu_2 = 2.82\ .10^{-4}\ kgm^{-1}s^{-1}$ and $\mu_3 = 1.8\ .10^{-5}\ kgm^{-1}s^{-1}$ are the dynamic viscosity of respectively the liquid water and liquid vapour at 1 bar and 293K. It is the limit of the closure law proposed in [17] for small diameter droplets.

- Temperature relaxation time scales:

$$\frac{1}{\tau_{12}^T} = \frac{1}{\tau_{21}^T} = \frac{6\alpha_1 Nu_1 \lambda_1 (m_1 C_{v_1} + m_2 C_{v_2})}{m_1 C_{v_1} m_2 C_{v_2} D_1^2} \; ; \tag{118}$$

$$\frac{1}{\tau_{13}^T} = \frac{1}{\tau_{31}^T} = \frac{6\alpha_1 Nu_1 \lambda_1 (m_1 C_{v_1} + m_3 C_{v_3})}{m_1 C_{v_1} m_3 C_{v_3} D_1^2} \; ; \tag{119}$$

$$\frac{1}{\tau_{23}^T} = \frac{1}{\tau_{32}^T} = \frac{6\alpha_3 Nu_3 \lambda_3 (m_2 C_{v_2} + m_3 C_{v_3})}{m_2 C_{v_2} m_3 C_{v_3} D_3^2} \; . \tag{120}$$

$$\tag{121}$$

where $Nu_1 = 10$, $Nu_3 = 10$ are the Nusselt number of the corium and the water vapour respectively and $\lambda_1 = 230$ $(Wm^{-1}K^{-1})$ and $\lambda_2 = 0.6$ $(Wm^{-1}K^{-1})$ are the thermal conductivity of the corium and liquid vapour respectively. This form is taken from [41, 40].

- Gibbs potential relaxation time scale τ_{23}^m is supposed to be constant:

$$\tau_{23}^m = \tau^m = 10^{-5} s \; . \tag{122}$$

Coefficient Γ_0 is here taken as:

$$\Gamma_0 = \max_{x \in]2.15,3.75[} \left(\left| m_3^0 (\gamma_2 C_{v_2} + \frac{\epsilon_{2_0}}{T_2^0}(2 + \frac{\epsilon_{2_0}}{C_{v_2} T_2^0})) + m_2^0 (\gamma_3 C_{v_3} + \frac{\epsilon_{3_0}}{T_3^0}(2 + \frac{\epsilon_{3_0}}{C_{v_3} T_3^0})) \right| (x) \right) . \tag{123}$$

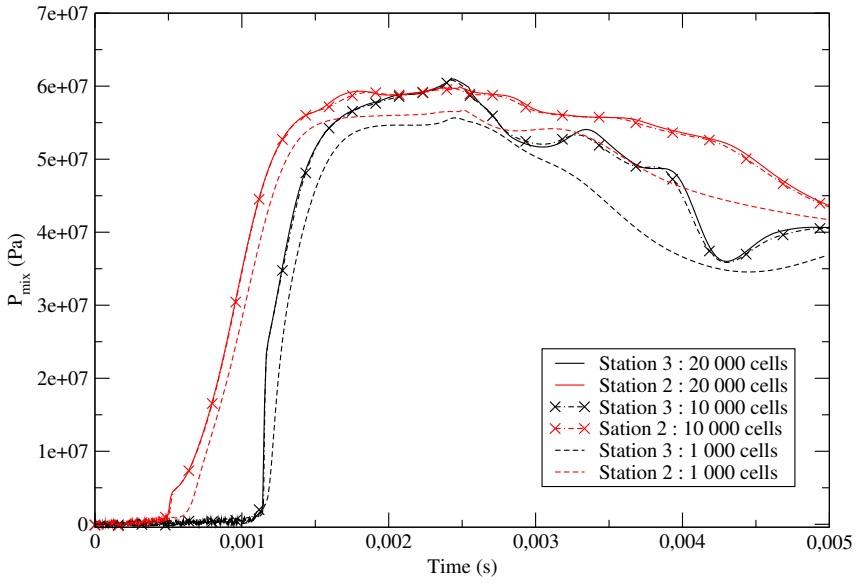

Figure 7: Evolution of the total pressure on station 2 (red lines) and 3 (black lines) for two meshes including respectively 1000 cells and 10 000 cells.

As we can see on **Figure** 7, the total pressure $P_{mix} = \sum_{k=1}^{3} \alpha_k P_k$ peaks at station 3 at $60,9$ MPa, which is close to the measured total pressure interval in [32] (50 MPa to 60 MPa). A similar test case has been computed in [6] but as the relaxation is supposed to be instantaneous for both pressure and velocity, the pressure peak was far lower than the one computed here. We note that, oscillations come up at the

beginning of the simulation, especially at station 3. Those oscillations occur as eigenvalues of the relaxation matrix $\mathscr{R}_{thermo}$ become complex conjugate. The coarse mesh can hardly capture the structure after the shock. The difference on the total pressure plateau between the two refined meshes (respectively 10 000 cells and 20 000 cells) is about 2% for station 3 and 1% for station 2.

Eventually, as shown in **Figure** 8, the droplet break-up is active throughout the simulation.

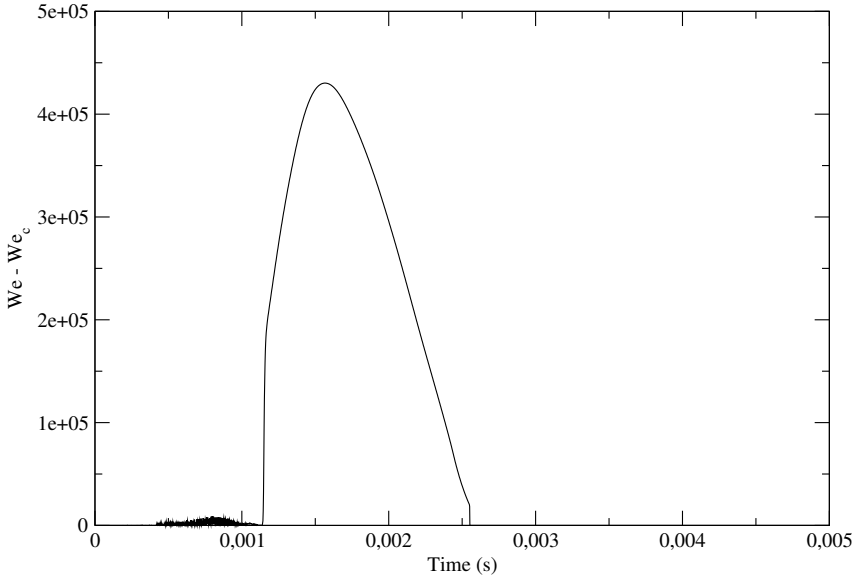

Figure 8: Evolution of the difference $We - We_c$ at station 3 with a mesh including 10 000 cells

5 Conclusion:

When tackling vapour explosion applications, we may conclude that the algorithms presented in this article, in order to account for source terms, enable us to obtain convergent approximations of solutions of the three-phase flow model [25, 24], when the mesh is refined. We recall here that the former algorithms detailed in reference [6] lead to a failure of the computer code, in a similar framework.

Obviously, the temptation is now great to extend the relaxation schemes developed in [11] for the convective effect of the two-phase flow model [1] (respectively for a barotropic three-phase flow in [44]), to the immiscible three-phase flow models with energy [25]. The reader is referred to [11] for a comparison of the capabilities of schemes introduced in [45] and [46], when focusing on the two-phase flow model [1].

Moreover, more complex/realistic EoS might be considered in the second step on the algorithm, instead of the simple SGG EoS considered herein. In that case, it would however remain to prove that existence and uniqueness of the discrete solution of step 2 (in the admissible state space) would hold true.

Eventually, the authors emphasize again that in this work, no strong assumption on the relaxation time scales underlies the model (such as in [16, 36, 15] for the two-phase flow framework), or the treatment of the source terms (as in [39, 22, 38] for the two-phase flow framework). However, beyond this, it urges the question of the accurate modeling of those relaxation time scales, and more generally the question of the modeling of the source terms. Actually, few closure laws for the two-phase flow framework exist in the literature, see for example [43, 33, 4, 17, 7]. Furthermore, we know that those time scales have a key role on the transient of the flow, see Figures 1, 3 and Appendix A in [34]. Therefore, a detailed parametric study on those relaxation time scales could lead to a better understanding of the inner relaxation process. Moreover, other source terms than the ones used in this paper have been proposed in the literature, and an attempt to compare some of them in the two-phase flow framework has been conducted in Chapter 2 of [8]. An extension of this study to the three-phase flow framework still remains to be achieved.

References

[1] Melvin R. Baer and Jace W. Nunziato. A two phase mixture theory for the deflagration to detonation transition (DDT) in reactive granular materials. *Int. J. Multiphase Flow*, 12-6:861–889, 1986.

[2] JB Bdzil, R Menikoff, SF Son, AK Kapila, and D Scott Stewart. Two-phase modeling of deflagration-to-detonation transition in granular materials: A critical examination of modeling issues. *Physics of fluids*, 11(2):378–402, 1999.

[3] Georges Berthoud. Vapor explosions. *Annual Review of Fluid Mechanics*, 32(1):573–611, 2000. Available at https://doi.org/10.1146/annurev.fluid.32.1.573.

[4] Zbigniew Bilicki and Joseph Kestin. Physical aspects of the relaxation model in two-phase flow. *Proceedings of the Royal Society of London. A. Mathematical and Physical Sciences*, 428(1875):379–397, 1990.

[5] Hamza Boukili and Jean-Marc Hérard. Relaxation and simulation of a barotropic three-phase flow model. *ESAIM: Math. Modeling and Numerical Analysis*, 53:1031–1059, 2019.

[6] Hamza Boukili and Jean-Marc Hérard. Simulation and preliminary validation of a three-phase flow model with energy. *Computers and Fluids*, 221:104868, 2021.

[7] Didier Bresch and Matthieu Hillairet. A compressible multifluid system with new physical relaxation terms. *Annales scientifiques de l' Ecole Normale Supérieure*, 52:255–295, 2019.

[8] Jean Bussac. *Modélisation et simulation d'écoulements multiphasiques avec phases miscibles*. Theses, Nantes Université, September 2023. https://theses.hal.science/tel-04232670.

[9] Alice Chauvin, Eric Daniel, Ashwin Chinnayya, Jacques Massoni, and Georges Jourdan. Shock waves in sprays: numerical study of secondary atomization and experimental comparison. *Shock Waves*, 26:403–415, 2016.

[10] Frédéric Coquel, Thierry Gallouët, Jean-Marc Hérard, and Nicolas Seguin. Closure laws for a two fluid two-pressure model. *Comptes Rendus Académie des Sciences Paris*, I-332:927–932, 2002.

[11] Frédéric Coquel, Jean-Marc Hérard, and Khaled Saleh. A positive and entropy-satisfying finite volume scheme for the Baer–Nunziato model. *Journal of Computational Physics*, 330:401–435, 2017.

[12] Fabien Crouzet, Frédéric Daude, Pascal Galon, Jean-Marc Hérard, Olivier Hurisse, and Yujie Liu. Validation of a two-fluid model on unsteady liquid-vapor water flows. *Computers and Fluids*, 119:131–142, 2015.

[13] Pedro Embid and Melvin R. Baer. Mathematical analysis of a two-phase continuum mixture theory. *Continuum Mechanics and Thermodynamics*, 4:279–312, 1992.

[14] Davide Ferrari, Ilya Peshkov, Evgeniy Romenski, and Michael Dumbser. A unified shtc multiphase model of continuum mechanics. *arXiv*, 2024. https://arxiv.org/pdf/2403.19298.

[15] Tore Flåtten and Gaute Linga. A hierarchy of non-equilibrium two-phase flow models. *ESAIM: Proceedings and Surveys*, 66:109–143, 2019.

[16] Tore Flåtten and Halvor Lund. Relaxation two-phase flow models and the sub-characteristic condition. *Mathematical Models and Methods in Applied Sciences*, 21:2379–2407, 2011.

[17] Sergey Gavrilyuk. The structure of pressure relaxation terms: the one-velocity case. *EDF report H-I83-2014-0276-EN*, 2014. Available upon request to: sergey.gavrilyuk@univ-amu.fr.

[18] Sergey Gavrilyuk. Uncertainty principle in two-fluid mechanics. *ESAIM: Proceedings and surveys*, 69:47–55, 2020.

[19] Sergey Gavrilyuk and Richard Saurel. Mathematical and numerical modeling of two-phase compressible flows with micro-inertia. *Journal of Computational Physics*, 175:326–360, 2002.

[20] Boris E. Gelfand. Droplet breakup phenomena in flows with velocity lag. *Progress in energy and combustion science*, 22(3):201–265, 1996.

[21] James Glimm, David Saltz, and David H. Sharp. Two phase flow modelling of a fluid mixing layer. *Journal of Fluid Mechanics*, 378:39–47, 1999.

[22] Lene Grabowsky, Maren Hantke, and Siegfried Müller. News on Baer–Nunziato type model at pressure equilibrium. *Continuum Mechanics and Thermodynamics*, 33:767–788, 2021.

[23] Maren Hantke and Siegfried Müller. Analysis and simulation of a new multi-component two-phase flow model with phase transition and chemical reactions. *Quarterly of Applied Mathematics*, 76, 2018.

[24] Maren Hantke, Siegfried Müller, and Pascal Richter. Closure conditions for non-equilibrium multi-component models. *Continuum Mechanics and Thermodynamics*, 28:1157–1189, 2016.

[25] Jean-Marc Hérard. A three-phase flow model. *Mathematical and Computer Modeling*, 45:732–755, 2007.

[26] Jean-Marc Hérard. A class of three-phase flow models with energy. *internal EDF report 6125-3016-2020-01853-EN*, 2020.

[27] Jean-Marc Hérard and Olivier Hurisse. A fractional step method to compute a class of compressible gas-liquid flows. *Computers and Fluids*, 55:57–69, 2012.

[28] Jean-Marc Hérard, Olivier Hurisse, and Lucie Quibel. A four-field three-phase flow model with both miscible and immiscible components. *Mathematical Modeling and Numerical Analysis*, 55:S251–S278, 2021.

[29] Jean-Marc Hérard and Guillaume Jomée. Two approaches to compute unsteady compressible two-phase flow models with stiff relaxation terms. *ESAIM: Mathematical Modelling and Numerical Analysis*, 57(6):3537–3583, 2023.

[30] Jean-Marc Hérard and Guillaume Jomée. Relaxation process in a hybrid two-phase flow model. *In revision*, 2024. https://hal.science/hal-04197280v2.

[31] Jean-Marc Hérard and Hélène Mathis. A three-phase flow model with two miscible phases. *Mathematical Modeling and Numerical Analysis*, 53:1373–1389, 2019.

[32] I Huhtiniemi, H Hohmann, R Faraoni, M Field, R Gambaretti, and K Klein. Krotos 38 to krotos 44: data report. *Technical Note No. I*, 96, 1996.

[33] Mamoru Ishii. Thermo-fluid dynamic theory of two-phase flow. *Eyrolles-Collection de la Direction des Etudes et Recherches EDF*, 1975.

[34] Guillaume Jomée. *Simulation of compressible non-equilibrium multiphase flow models*. Phd thesis, Aix-Marseile Université, November 2023. https://hal.science/tel-04338786.

[35] Ashwani Kapila, Steven F. Son, John B. Bdzil, Ralph Menikoff, and Donald S. Stewart. Two phase modeling of a DDT: structure of the velocity relaxation zone. *Physics of Fluids*, 9-12:3885–3897, 1997.

[36] Halvor Lund. A hierarchy of relaxation models for two-phase flow. *SIAM Journal on Applied Mathematics*, 72:1713–1741, 2012.

[37] Maxima. Maxima : A computer algebra system. https://maxima.sourceforge.io/.

[38] Marica Pelanti. Arbitrary-rate relaxation techniques for the numerical modeling of compressible two-phase flows with heat and mass transfer. *International Journal of Multiphase Flow*, 153, 2022.

[39] Marica Pelanti and Keh-Ming Shyue. A numerical model for multiphase liquid–vapor–gas flows with interfaces and cavitation. *International Journal of Multiphase Flow*, 113, 2019.

[40] Stéphane Picchi. *MC3D Version 3.9 : Description of the models of the premixing application*. IRSN internal report, 2017.

[41] Martin M. Pilch and CA Erdman. Use of breakup time data and velocity history data to predict the maximum size of stable fragments for acceleration-induced breakup of a liquid drop. *International journal of multiphase flow*, 13(6):741–757, 1987.

[42] Pratik Rai. *Modeling and numerical simulation of compressible multicomponent flows*. PhD thesis, Institut Polytechnique de Paris, 2021. Available at : https://tel.archives-ouvertes.fr/tel-03461287.

[43] William E. Ranz. Evaporation from drops-i and-ii. *Chem. Eng. Progr*, 48:141–146, 1952.

[44] Khaled Saleh. A relaxation scheme for a hyperbolic multiphase flow model-part i: Barotropic eos. *ESAIM: Mathematical Modelling and Numerical Analysis*, 53(5):1763–1795, 2019.

[45] Donald W. Schwendeman, Christopher W. Wahle, and Ashwana K. Kapila. The Riemann problem and a high-resolution Godunov method for a model of compressible two-phase flow. *Journal of Computational Physics*, 212(2):490–526, 2006.

[46] Svetlana A. Tokareva and Eleuterio F. Toro. HLLC-type Riemann solver for the Baer–Nunziato equations of compressible two-phase flow. *Journal of Computational Physics*, 229(10):3573–3604, 2010.

Appendix 1: Numerical parameters

	Phase 1	Phase 2	Phase 3
C_v	1.2872948262582229e+01	1.452904592629688e+03	4.441148752333071e+03
γ	2.2838590974110350e+01	1.614924811807376e+00	1.085507894797296e+00
$\hat{\Pi}$	1.8847923625716622e+09	3.563521398523755e+08	0.0
ϵ_0	-1.3316200000000000e+05	0.0	0.0
s_0	0.0	0.0	-4.769786773517021e+04

Table 1: EoS coefficients for all of the conducted simulations

$P_1(t=0)$	1.0 bar
$P_2(t=0)$	1.0 bar
$P_3(t=0)$	1.0 bar
$T_1(t=0)$	2500.0 K
$T_2(t=0)$	363.0 K
$T_3(t=0)$	1000.0 K
$\alpha_1(t=0)$	0.026
$\alpha_2(t=0)$	0.884
$\alpha_3(t=0)$	0.09

Table 2: Initial conditions for the homogeneous cases

	Case A	Case B
τ^P	1.0e-5 s	1.0e-8 s
τ^T	1.0e-3 s	1.0e-3 s
τ^m	1.0e-2 s	1.0e-2 s

Table 3: Numerical parameters for Case A and Case B in the homogeneous case.

Appendix 2: Coefficients of the relaxation matrix

First, we define $\mathscr{R}^{relax}$ as:

$$\mathscr{R}^{relax}(W) = \begin{pmatrix} R_{UU}(W) & 0 & 0 & 0 \\ R_{PU}(W) & R_{PP}(W) & R_{PT}(W) & r_{Pg}(W) \\ R_{TU}(W) & R_{TP}(W) & R_{TT}(W) & r_{Tg}(W) \\ r_{gU}(W)^\intercal & r_{gP}(W)^\intercal & r_{gT}(W)^\intercal & r_g(W) \end{pmatrix}. \tag{124}$$

Matrices $R_{UU}(W)$, $R_{PU}(W)$, R_{PP}, $R_{PT}(W)$, $R_{TU}(W)$, $R_{TP}(W)$, $R_{TT}(W)$ are in $\mathscr{M}_2(\mathbb{R})$, whereas $r_{Pg}(W)$, $r_{Tg}(W)$, $r_{gU}(W)$, $r_{gP}(W)$, r_{gT} are in $\mathbb{R}^2$ and r_g is a scalar. Coefficients of $R_{UU}(W)(W)$ write as follows:

$$\begin{aligned} r_{UU_{11}} &= \frac{1}{m_1} d_{12} + \frac{1}{m_2}\left(d_{12} + d_{23} - \frac{\Lambda_{23}}{2}\Delta g_{23} \right) , \\ r_{UU_{12}} &= \frac{1}{m_1} d_{13} - \frac{1}{m_2}\left(d_{23} - \frac{\Lambda_{23}}{2}\Delta g_{23} \right) , \\ r_{UU_{21}} &= \frac{1}{m_1} d_{12} - \frac{1}{m_3}\left(d_{23} + \frac{\Lambda_{23}}{2}\Delta g_{23} \right) , \\ r_{UU_{22}} &= \frac{1}{m_1} d_{13} + \frac{1}{m_3}\left(d_{13} + d_{23} + \frac{\Lambda_{23}}{2}\Delta g_{23} \right) . \end{aligned} \tag{125}$$

Writing $\theta_k = m_k \left.\dfrac{\partial \epsilon_k}{\partial T_k}\right|_{\rho_k}$, and:

$$\begin{aligned} F_{21} &= K_{12}\rho_1^2 \left.\frac{\partial \epsilon_1}{\partial \rho_1}\right|_{T_1} - P_2 K_{12} + (\Delta P_{12} - \Delta P_{13}) K_{23} , \\ F_{31} &= K_{13}\rho_1^2 \left.\frac{\partial \epsilon_1}{\partial \rho_1}\right|_{T_1} - P_3 K_{13} - (\Delta P_{12} - \Delta P_{13}) K_{23} , \\ F_{22} &= -(K_{12} + K_{23})\rho_2^2 \left.\frac{\partial \epsilon_2}{\partial \rho_2}\right|_{T_2} + P_2 (K_{23} + K_{12}) , \\ F_{32} &= K_{23}\rho_2^2 \left.\frac{\partial \epsilon_2}{\partial \rho_2}\right|_{T_2} - P_2 K_{23} , \\ F_{23} &= K_{23}\rho_3^2 \left.\frac{\partial \epsilon_3}{\partial \rho_3}\right|_{T_3} - P_3 K_{23} , \\ F_{33} &= -(K_{13} + K_{23})\rho_3^2 \left.\frac{\partial \epsilon_3}{\partial \rho_3}\right|_{T_3} + P_3 (K_{23} + K_{13}) . \end{aligned}$$

Moreover, setting $\sigma_k = m_k \left.\dfrac{\partial \epsilon_k}{\partial P_k}\right|_{\rho_k}$, and:

$$\begin{aligned} G_{21} &= -K_{12}(\rho_1 c_1)^2 \left.\frac{\partial \epsilon_1}{\partial P_1}\right|_{\rho_1} + \Delta P_{12} K_{12} + (\Delta P_{12} - \Delta P_{13}) K_{23} , \\ G_{31} &= -K_{13}(\rho_1 c_1)^2 \left.\frac{\partial \epsilon_1}{\partial P_1}\right|_{\rho_1} + \Delta P_{13} K_{13} - (\Delta P_{12} - \Delta P_{13}) K_{23} , \\ G_{22} &= (K_{12} + K_{23})(\rho_2 c_2)^2 \left.\frac{\partial \epsilon_2}{\partial P_2}\right|_{\rho_2} , \\ G_{32} &= -K_{23}(\rho_2 c_2)^2 \left.\frac{\partial \epsilon_2}{\partial P_2}\right|_{\rho_2} , \\ G_{23} &= -K_{23}(\rho_3 c_3)^2 \left.\frac{\partial \epsilon_3}{\partial P_3}\right|_{\rho_3} , \\ G_{33} &= (K_{13} + K_{23})(\rho_3 c_3)^2 \left.\frac{\partial \epsilon_3}{\partial P_3}\right|_{\rho_3} . \end{aligned}$$

Coefficients of the sub-matrices of $\mathscr{R}^{relax}(W)$ read:

- $R_{TU}(W) =$

$$r_{TU_{11}} = \Delta U_{12}\left(\frac{d_{12}+d_{23}}{2\theta_2} - \frac{d_{12}}{2\theta_1}\right) - \frac{d_{23}}{2\theta_2}\Delta U_{13} \ , \tag{126}$$

$$r_{TU_{12}} = \Delta U_{13}\left(\frac{d_{23}}{2\theta_2} - \frac{d_{13}}{2\theta_1}\right) - \frac{d_{23}}{2\theta_2}\Delta U_{12} \ , \tag{127}$$

$$r_{TU_{21}} = \Delta U_{12}\left(\frac{d_{23}}{2\theta_3} - \frac{d_{12}}{2\theta_1}\right) - \frac{d_{23}}{2\theta_3}\Delta U_{13} \ , \tag{128}$$

$$r_{TU_{22}} = \Delta U_{13}\left(\frac{d_{13}+d_{23}}{2\theta_3} - \frac{d_{13}}{2\theta_1}\right) - \frac{d_{23}}{2\theta_3}\Delta U_{12} \ . \tag{129}$$

$$\tag{130}$$

- $R_{TP}(W) =$

$$r_{TP_{11}} = -\frac{F_{21}}{\theta_1} + \frac{F_{22}}{\theta_2} \ , \tag{131}$$

$$r_{TP_{12}} = -\frac{F_{31}}{\theta_1} + \frac{F_{32}}{\theta_2} \ , \tag{132}$$

$$r_{TP_{21}} = -\frac{F_{21}}{\theta_1} + \frac{F_{23}}{\theta_3} \ , \tag{133}$$

$$r_{TP_{22}} = -\frac{F_{31}}{\theta_1} + \frac{F_{33}}{\theta_3} \ . \tag{134}$$

$$\tag{135}$$

- $R_{TT}(W) =$

$$r_{TT_{11}} = \frac{q_{12}}{\theta_1} + \frac{q_{12}+q_{23}}{\theta_2} \ , \tag{136}$$

$$r_{TT_{12}} = \frac{q_{13}}{\theta_1} - \frac{q_{23}}{\theta_2} \ , \tag{137}$$

$$r_{TT_{21}} = -\frac{q_{23}}{\theta_3} + \frac{q_{12}}{\theta_1} \ , \tag{138}$$

$$r_{TT_{22}} = \frac{q_{13}}{\theta_1} + \frac{q_{13}+q_{23}}{\theta_3} \ . \tag{139}$$

$$\tag{140}$$

- $r_{Tg}(W) =$

$$r_{Tg_1} = \frac{\Lambda_{23}}{\theta_2}\left(\epsilon_2 + \rho_2 \left.\frac{\partial \epsilon_2}{\partial \rho_2}\right|_{T_2}\right) \ , \tag{141}$$

$$r_{Tg_2} = -\frac{\Lambda_{23}}{\theta_3}\left(\epsilon_3 + \rho_3 \left.\frac{\partial \epsilon_3}{\partial \rho_3}\right|_{T_3}\right) \ . \tag{142}$$

$$\tag{143}$$

- $R_{PU}(W) =$

$$r_{PU_{11}} = \Delta U_{12}\left(\frac{d_{12}+d_{23}}{2\sigma_2} - \frac{d_{12}}{2\sigma_1}\right) - \frac{d_{23}}{2\sigma_2}\Delta U_{13} \ , \tag{144}$$

$$r_{PU_{12}} = \Delta U_{13}\left(\frac{d_{23}}{2\sigma_2} - \frac{d_{13}}{2\sigma_1}\right) - \frac{d_{23}}{2\sigma_2}\Delta U_{12} \ , \tag{145}$$

$$r_{PU_{21}} = \Delta U_{12}\left(\frac{d_{23}}{2\sigma_3} - \frac{d_{12}}{2\sigma_1}\right) - \frac{d_{23}}{2\sigma_3}\Delta U_{13} \ , \tag{146}$$

$$r_{PU_{22}} = \Delta U_{13}\left(\frac{d_{13}+d_{23}}{2\sigma_3} - \frac{d_{13}}{2\sigma_1}\right) - \frac{d_{23}}{2\sigma_3}\Delta U_{12} \ . \tag{147}$$

$$\tag{148}$$

- $R_{PP}(W) =$

$$r_{PP_{11}} = \frac{1}{m_1}\left((\rho_1 c_1)^2 K_{12} + (\left.\frac{\partial \epsilon_1}{\partial P_1}\right|_{\rho_1})^{-1}(K_{23}\Delta P_{13} - (K_{12}+K_{23})\Delta P_{12})\right) + \frac{1}{m_2}(\rho_2 c_2)^2(K_{12}+K_{23}) \ , \tag{149}$$

$$r_{PP_{12}} = \frac{1}{m_1}\left(K_{13}(\rho_1 c_1)^2 + (\left.\frac{\partial \epsilon_1}{\partial P_1}\right|_{\rho_1})^{-1}(K_{23}\Delta P_{12} - (K_{23}+K_{13})\Delta P_{13})\right) - \frac{1}{m_2}K_{23}(\rho_2 c_2)^2 \ , \tag{150}$$

$$r_{PP_{21}} = \frac{1}{m_1}\left((\rho_1 c_1)^2 K_{12} + (\left.\frac{\partial \epsilon_1}{\partial P_1}\right|_{\rho_1})^{-1}(K_{23}\Delta P_{13} - (K_{12}+K_{23})\Delta P_{12})\right) - \frac{1}{m_3}K_{23}(\rho_3 c_3)^2 \ , \tag{151}$$

$$r_{PP_{22}} = \frac{1}{m_1}\left(K_{13}(\rho_1 c_1)^2 + (\left.\frac{\partial \epsilon_1}{\partial P_1}\right|_{\rho_1})^{-1}(K_{23}\Delta P_{12} - (K_{23}+K_{13})\Delta P_{13})\right) + \frac{1}{m_3}(K_{13}+K_{23})(\rho_3 c_3)^2 \ . \tag{152}$$

$$\tag{153}$$

- $R_{PT}(W) =$

$$r_{PT_{11}} = \frac{q_{12}}{\sigma_1} + \frac{q_{12}+q_{23}}{\sigma_2} \ , \tag{154}$$

$$r_{PT_{12}} = \frac{q_{13}}{\sigma_1} - \frac{q_{23}}{\sigma_2} \ , \tag{155}$$

$$r_{PT_{21}} = -\frac{q_{23}}{\sigma_3} + \frac{q_{12}}{\sigma_1} \ , \tag{156}$$

$$r_{PT_{22}} = \frac{q_{13}}{\sigma_1} + \frac{q_{13}+q_{23}}{\sigma_3} \ . \tag{157}$$

$$\tag{158}$$

- $r_{Pg}(W) =$

$$r_{Pg_1} = \frac{\Lambda_{23}}{\sigma_2}\left(\epsilon_2 + \frac{P_2}{\rho_2} - \rho_2 c_2^2 \left.\frac{\partial \epsilon_2}{\partial P_2}\right|_{\rho_2}\right) \ , \tag{159}$$

$$r_{Pg_2} = -\frac{\Lambda_{23}}{\sigma_3}\left(\epsilon_3 + \frac{P_3}{\rho_3} - \rho_3 c_3^2 \left.\frac{\partial \epsilon_3}{\partial P_3}\right|_{\rho_3}\right) \ . \tag{160}$$

$$\tag{161}$$

- $r_{gU}(W) =$

$$r_{gU_1} = -\frac{1}{2\rho_2 T_2}\left(\frac{1}{\sigma_2} - \frac{\rho_2 h_2}{\theta_2}\right)\left[d_{12}\Delta U_{12} + d_{23}(\Delta U_{12} - \Delta U_{13})\right] + \frac{d_{23}}{2\rho_3 T_3}\left(\frac{1}{\sigma_3} - \frac{\rho_3 h_3}{\theta_3}\right)\left[\Delta U_{12} - \Delta U_{13}\right] \ , \tag{162}$$

$$r_{gU_2} = -\frac{d_{23}}{2\rho_2 T_2}\left(\frac{1}{\sigma_2} - \frac{\rho_2 h_2}{\theta_2}\right)(\Delta U_{12} - \Delta U_{13}) + \frac{1}{2\rho_3 T_3}\left(\frac{1}{\sigma_3}\frac{\rho_3 h_3}{\theta_3}\right)\left[d_{13}\Delta U_{13} + d_{23}(\Delta U_{13} - \Delta U_{12})\right] \ . \tag{163}$$

$$\tag{164}$$

- $r_{gP}(W) =$

$$r_{gP_1} = -\frac{1}{\rho_2 T_2}\left(\frac{G_{22}}{\sigma_2} - \frac{\rho_2 h_2 F_{22}}{\theta_2 T_2}\right) + \frac{1}{\rho_3 T_3}\left(\frac{G_{23}}{\sigma_3} - \frac{\rho_3 h_3 F_{23}}{\theta_3 T_3}\right) , \tag{165}$$

$$r_{gP_2} = -\frac{1}{\rho_2 T_2}\left(\frac{G_{32}}{\sigma_2} - \frac{\rho_2 h_2 F_{32}}{\theta_2 T_2}\right) + \frac{1}{\rho_3 T_3}\left(\frac{G_{33}}{\sigma_3} - \frac{\rho_3 h_3 F_{33}}{\theta_3 T_3}\right) . \tag{166}$$

$$\tag{167}$$

- $r_{gT}(W) =$

$$r_{gT_1} = -\frac{1}{\rho_2 T_2}\left(\frac{1}{\sigma_2} - \frac{\rho_2 h_2}{\theta_2 T_2}\right)(q_{12} + q_{23}) - \frac{q_{23}}{\rho_3 T_3}\left(\frac{1}{\sigma_3} - \frac{\rho_3 h_3}{\theta_3 - T_3}\right) , \tag{168}$$

$$r_{gT_2} = \frac{q_{23}}{\rho_2 T_2}\left(\frac{1}{\sigma_2} - \frac{\rho_2 h_2}{\theta_2 T_2}\right) + \frac{1}{\rho_3 T_3}\left(\frac{1}{\sigma_3} - \frac{\rho_3 h_3}{\theta_3 T_3}\right)(q_{13} + q_{23}) . \tag{169}$$

$$\tag{170}$$

- $r_g(W) =$

$$\begin{aligned} &- \Lambda_{23}[\frac{1}{\rho_2 T_2}\left(\frac{h_2}{\sigma_2} - \frac{\rho_2 c_2^2}{\sigma_2}\left.\frac{\partial \epsilon_2}{\partial P_2}\right|_{\rho_2} - \frac{\rho_2 h_2}{\theta_2 T_2}\left(\epsilon_2 + \rho_2 \left.\frac{\partial \epsilon_2}{\partial \rho_2}\right|_{T_2}\right)\right) \\ &+ \frac{1}{\rho_3 T_3}\left(\frac{h_3}{\sigma_3} - \frac{\rho_3 c_3^2}{\sigma_3}\left.\frac{\partial \epsilon_3}{\partial P_3}\right|_{\rho_3} - \frac{\rho_3 h_3}{\theta_3 T_3}\left(\epsilon_3 + \rho_3 \left.\frac{\partial \epsilon_3}{\partial \rho_3}\right|_{T_3}\right)\right)] \end{aligned} \tag{171}$$

Appendix 3: Velocity relaxation algorithm

The sub-system that characterizes this step can be written as follows:

$$\begin{cases} \partial_t \alpha_k = 0 \\ \partial_t m_k = 0 \\ \partial_t \left(m_k U_k\right) = -\sum\limits_{l=1, l\neq k}^{3} d_{kl}(W)\Delta U_{kl} \\ \partial_t \left(\alpha_k E_k\right) = -\sum\limits_{l=1, l\neq k}^{3} V_{kl}(W)\cdot d_{kl}(W)\Delta U_{kl} \end{cases} \tag{172}$$

From (172), one can obtain the following equation:

$$\partial_t \Delta U = -\hat{R}_{UU}\Delta U, \tag{173}$$

with $\hat{R}_{UU} \in M_2(\mathbb{R})$ that corresponds to the matrix R_{UU} of (125) with $\Delta g_{23} = 0$;

The algorithm used for computing approximate solutions for the velocity relaxation step is identical to Algorithm 3.3.1.2 presented in [6]. It consists, on each cell of the mesh, in five steps:

- **Step 1:** Initialize the vector of velocity differences at time t^{n-} (right after the convective step): $\Delta U^{n-} = (\Delta U_{12}^{n-}, \Delta U_{13}^{n-})^\intercal$ and matrix $\hat{R}_{UU}$ at time t^{n-}.
- **Step 2:** Compute ΔU^n such as:

$$\left(\mathscr{I} + \Delta t_n \hat{R}_{UU}(W^{n-})\right)\Delta U^n = \Delta U^{n-} , \tag{174}$$

  with $\mathscr{I}$ the identity matrix in $M_2(\mathbb{R})$.

- **Step 3:** Compute U_1^n using the total momentum conservation:

$$U_1^n = \frac{\sum_{k=1}^{3} \left(m_k \mathbf{U}_k\right)^{n-} + m_2^{n-} \Delta U_{12}^n + m_3^{n-} \Delta U_{13}^n}{\left(m_1 + m_2 + m_3\right)^{n-}} \ . \tag{175}$$

- **Step 4:** Update U_2^n and U_3^n as:

$$U_2^n = U_1^n - \Delta U_{12}^n \quad ; \quad U_3^n = U_1^n - \Delta U_{13}^n \ . \tag{176}$$

- **Step 5:** Update the total energy by integrating the evolution equation of the total energy of system (172):

$$\left(\alpha_k E_k\right)^n = \left(\alpha_k E_k\right)^{n-} - \Delta t \sum_{l=1, l\neq k}^{3} \frac{d_{kl}\left(W^{n-}\right)}{2} \left(\left(U_k^n\right)^2 - \left(U_l^n\right)^2 \right) \tag{177}$$

Appendix 4: Interfacial area

The definition of an interfacial area $\mathscr{A}_1$ for the phase 1 (corium) is needed in order to capture the behaviour of the solution [20, 3, 9]:

$$\mathscr{A}_1 = \frac{6\alpha_1}{D_1} \tag{178}$$

Its equation of evolution is supposed to be:

$$\frac{\partial \mathscr{A}_1}{\partial t} + \nabla(\mathscr{A}_1 U_1) = g(\mathscr{A}_1, W); \tag{179}$$

with, see [5, 41]:

$$g(\mathscr{A}_1, W) = C_0 \frac{\mathscr{A}_1^2}{6\alpha_1} (\frac{\rho_1}{\rho_2})^{1/2} \|U_1 - U_2\| f(We); \tag{180}$$

where the coefficient $C_0 = 0.245$ and We the Weber number is defined as follows:

$$We = \frac{\rho_1 \|U_1 - U_2\|^2 D_1}{\sigma_1} \tag{181}$$

with $\sigma_1 = 73\ .10^{-3} (N.m^{-1})$ a reference surface tension [40] . Moreover f(We) is defined as:

$$f(We) = 1 \ , \ if \ \ We > We_c \ ; \ f(We) = 0 \ otherwise \tag{182}$$

where $We_c = 12$ is called the critical Weber number.

Adding this new equation does not change the structure and properties of the global system (6) according to [5]. Hence, it is chosen for the simulation. The numerical scheme used to simulate (179) is detailed in [5]. It consists of an explicit implicit step method, splitting the convective part and the source term part. Those two steps will respectively be inserted inside the explicit simulation step of the convective part of system (6) and the implicit simulation of the source terms of the same system.